Chapter III

Comparison of heat and moisture fluxes from a modified soil-plant-atmosphere model with observations from BOREAS

JOURNAL OF GEOPHYSICAL RESEARCH, VOL. 109, D08103, doi:10.1029/2003JD003949, 2004

Comparison of heat and moisture fluxes from a modified soil-plant-atmosphere model with observations from BOREAS

Young-Hee Lee[1] and L. Mahrt

College of Oceanic and Atmospheric Sciences, Oregon State University, Corvallis, Oregon, USA

Received 3 July 2003; revised 17 February 2004; accepted 23 February 2004; published 21 April 2004.

[1] This study evaluates the prediction of heat and moisture fluxes from a new land surface scheme with eddy correlation data collected at the old aspen site during the Boreal Ecosystem-Atmosphere Study (BOREAS) in 1994. The model used in this study couples a multilayer vegetation model with a soil model. Inclusion of organic material in the upper soil layer is required to adequately simulate exchange between the soil and subcanopy air. Comparisons between the model and observations are discussed to reveal model misrepresentation of some aspects of the diurnal variation of subcanopy processes. *INDEX TERMS:* 1878 Hydrology: Water/energy interactions; 1818 Hydrology: Evapotranspiration; 3322 Meteorology and Atmospheric Dynamics: Land/atmosphere interactions; *KEYWORDS:* evapotranspiration, canopy model, organic soil layer, BOREAS

Citation: Lee, Y.-H., and L. Mahrt (2004), Comparison of heat and moisture fluxes from a modified soil-plant-atmosphere model with observations from BOREAS, *J. Geophys. Res.*, *109*, D08103, doi:10.1029/2003JD003949.

1. Introduction

[2] Modeling approaches for surface fluxes of heat, moisture and carbon dioxide can be classified into single-source models, two-source models and multilayer models. In the single-source model, evaporation is determined as if the plant canopy were a partly wet plane at the lower boundary of the atmosphere using bulk aerodynamic resistance and stomatal resistance. The bulk stomatal resistance in the single-source model is less well behaved than leaf stomatal resistance in two-source or multilevel models since it is not a purely physiological parameter [*Raupach and Finnigan*, 1988]. Results from single-source models can be particularly sensitive to the roughness lengths for heat and moisture, which can behave erratically over vegetated surfaces.

[3] In two-source models [*Kustas*, 1990; *Sellers et al.*, 1986; *Choudhury and Monteith*, 1988; *Norman et al.*, 1995], an explicit single vegetation layer is considered separately from the ground surface. Although this model is more realistic than the single-source model, vertical structure of the canopy is not resolved. In actual canopies, the stomatal resistance depends significantly on height within the canopy because radiation, turbulence transfer and water supply from the root system vary with height. Consequently, multilayer models have been developed to simulate tall canopies such as forests [*Su et al.*, 1996; *Albertson et al.*, 2001]. These models aim to describe not only the evaporation from the entire canopy, but also the partitioning of the evapotranspiration between various parts of the canopy together with other aspects of the canopy microclimate such as profiles of leaf and air temperature and air humidity. The price of such details is more complexity and parameter input requirements. The choice of model complexity depends on the purpose and availability of computer resources.

[4] Even when multilevel canopy models approximate the actual canopy processes, the coupling between the atmospheric boundary layer and canopy models requires estimation of aerodynamic quantities [*Sun et al.*, 1999] and compliance with Monin-Obukhov similarity theory. In the roughness sublayer immediately above the canopy, the flux-gradient relationship based upon Monin-Obukhov similarity theory can significantly underestimate scalar fluxes [*Simpson et al.*, 1998; *Kaimal and Finnigan*, 1994]. Parameterizations for the roughness sublayer [*Cellier and Brunet*, 1991; *Wenzel et al.*, 1997; *Physick and Garratt*, 1995] are difficult to verify from observations, partly because of the potentially large horizontal gradients on the scale of the roughness elements [e.g., *Katul et al.*, 1999]. Such microscale heterogeneity can contribute to vertical flux divergence due to increasing footprint with height. Two-source models apply Monin-Obukhov similarity theory by assuming that the aerodynamic temperature for Monin-Obukhov similarity is equal to the canopy air temperature. Although this simplification can lead to significant errors [*Sun et al.*, 1999], alternative procedures have not been developed and we employ the same approximation in this study.

[5] The canopy turbulence is driven partly by coherent eddies of canopy scale sometimes leading to locally countergradient fluxes [*Raupach et al.*, 1996]. Existing numerical models of canopy turbulence span a wide range of complexities from K theory to higher order closure modeling and LES modeling [*Katul and Albertson*, 1998; *Shaw and Schumann*, 1992]. Although K theory does not describe countergradient fluxes, for practical purposes, K theory remains an adequate approximation for some applications [*Dolman and Wallace*, 1991] and is still used in many large-scale models [*Bonan*, 1996; *Cotton et al.*, 2003].

[1]Now at Department of Astronomy and Atmospheric Sciences, Kyungpook National University, Daegu, Republic of Korea.

0148-0227/04/2003JD003949$09.00

[6] The coupling between the canopy air and soil through fluxes of heat and moisture can be governed by a shallow soil layer of high organic content above the mineral soil [*Pauwels and Wood*, 1999a; *Van de Wiel et al.*, 2002]. The organic layer is not usually included in soil models. *Blanken et al.* [1997] and others have noted that leaf litter on the forest floor can act as a quasi-insulator and therefore promote large subsurface temperature gradients in addition to greater daytime warming of the subcanopy air in the pre-leaf-out period. More specifically, the soil surface layer with high organic content is normally characterized by smaller thermal conductivity and high porosity compared to mineral soils [*Letts et al.*, 2000]. *Pauwels and Wood* [1999a, 1999b, 2000] also pointed out the importance of an organic surface layer and included an organic surface layer in TOPLATS. The model performed well in simulating surface fluxes above the canopy but slightly overestimated the ground heat flux during the course of the day [*Pauwels and Wood*, 1999b] in BOREAS [*Sellers et al.*, 1995]. Although the modeled ground heat flux is sensitive to parameters such as moss thickness, thermal conductivity and heat capacity [*Pauwels and Wood*, 1999b], subcanopy turbulence also plays an important role in determining ground heat flux. In this study, we focus on evaluation of the subcanopy flux and interaction between the surface organic layer and the subcanopy air.

[7] To examine the interaction between microclimate and physiology, we have coupled the multilevel canopy model of *Williams et al.* [1996] with a soil model and atmospheric boundary layer model for use in regional models. This study evaluates the offline performance of the canopy and soil models in terms of vertical structure within the canopy and interaction with an organic surface layer. The model will be compared with data collected at the old aspen site during BOREAS.

2. Model

[8] The land surface model is based on the canopy model (soil plant atmosphere (SPA) model) of *Williams et al.* [1996, 2001], coupled to a multilayer soil model with snow and frozen soil physics [*Mahrt and Pan*, 1984; *Koren et al.*, 1999; *Peters-Lidard et al.*, 1998] and the surface runoff scheme of *Schaake et al.* [1996]. The canopy model computes the stomatal resistance in each canopy layer to maximize daily carbon gain per unit leaf nitrogen content, within the limitation of canopy water storage and transport of water from soil to the canopy [*Williams et al.*, 1996]. The radiation routines model the incidence, interception, absorption and reflectance of PAR (Photosynthetic Active Radiation), near infrared radiation (NIR) and longwave radiation in each canopy layer [*Amthor*, 1994; *Amthor et al.*, 1994]. A spherical leaf angle distribution is assumed.

[9] Here we apply two vegetation layers with the same thickness. Four soil layers are employed with thicknesses of 0.1, 0.3, 0.6 and 1 m, where the top layer includes organic material. We refer to the above papers for a description of the model components and here describe only parts of the model where changes are made.

2.1. Subcanopy Processes

[10] The total surface fluxes are partitioned into vegetation and ground components. Transport is formulated in terms of the atmospheric eddy diffusivities and leaf boundary layer resistances (Figure 1). The subcanopy air temperatures (T_1 and T_2) and the water vapor mixing ratios (q_1 and q_2) are calculated using the leaf temperature (T_{iv}), the saturation mixing ratio (q_{iv}) evaluated at the leaf temperature, the ground temperature (T_g), the ground saturation mixing ratio (q_g) for the ground temperature and resistances by solving the following equations for water vapor and temperature by iteration:

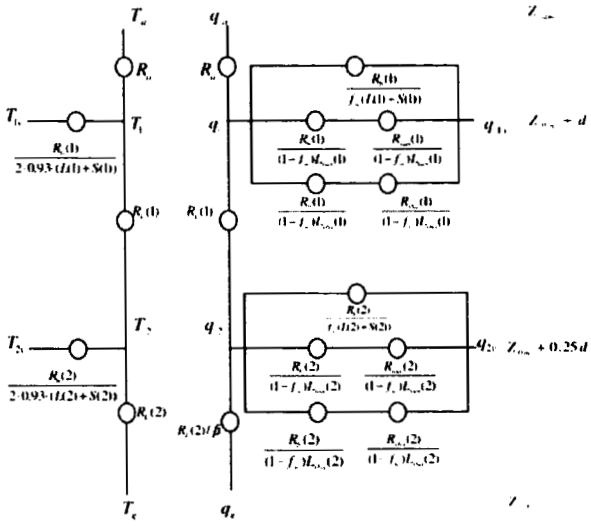

Figure 1. The transfer diagram for the canopy system.

$$\frac{q_a - q_1}{R_a} = \left[\frac{q_1 - q_{1v}}{R_b(1) + R_{sun}(1)} L_{sun}(1) + \frac{q_1 - q_{1v}}{R_b(1) + R_{sha}(1)} L_{sha}(1)\right] \cdot (1 - f_w) + \frac{q_1 - q_{1v}}{R_b(1)} f_w(L(1) + S(1)) + \frac{q_1 - q_2}{R_k(1)} \quad (1)$$

$$\frac{q_1 - q_2}{R_k(1)} = \left[\frac{q_2 - q_{2v}}{R_b(2) + R_{sun}(2)} L_{sun}(2) + \frac{q_2 - q_{2v}}{R_b(2) + R_{sha}(2)} L_{sha}(2)\right] \cdot (1 - f_w) + \frac{q_2 - q_{2v}}{R_b(2)} f_w(L(2) + S(2)) + \frac{q_2 - q_g}{R_k(2)/\beta} \quad (2)$$

$$\frac{T_a - T_1}{R_a} = \frac{2 \cdot 0.93(T_1 - T_{1v})}{R_b(1)} (L(1) + S(1)) + \frac{T_1 - T_2}{R_k(1)} \quad (3)$$

$$\frac{T_1 - T_2}{R_k(1)} = \frac{2 \cdot 0.93(T_2 - T_{2v})}{R_b(2)} (L(2) + S(2)) + \frac{T_2 - T_g}{R_k(2)}, \quad (4)$$

where q_a and T_a are the mixing ratio and the air temperature at the reference height (39 m from the ground) above the canopy, R_a is the aerodynamic resistance in the surface layer, R_k is the subcanopy resistance, R_b is the leaf boundary layer resistance and R_{sun} and R_{sha} are the stomatal resistance for sunlit and shaded leaf areas, respectively, f_w is the wet fraction of leaf and β is the soil wetness function (equation (13)). L_{sun} is the sunlit leaf area index, L_{sha} the

shaded leaf area index and L and S are the leaf area index and stem area index, respectively. While transpiration occurs on one side of the leaf, sensible heat flux occurs from both sides of the leaf due to mechanical mixing. Therefore a factor of 2 is used in equations (3)–(4). The value of 0.93 in equations (3) and (4) accounts for the differences in molecular diffusivities between heat and water vapor. It is assumed that the air adjacent to the shaded leaf surface is the same as that adjacent to the sunlit leaf surface due to sufficient mixing. Therefore no differentiation of leaf boundary layer resistance was made between shaded and sunlit leaf surfaces. The leaf temperature is calculated from the leaf energy balance equation. Neglecting any metabolic and physical storage, the leaf energy balance equation becomes

$$R_n = H_v + \lambda E_v(1 - f_w) + \lambda E_c f_w, \tag{5}$$

where H_v is the leaf sensible heat flux, R_n is the net radiation of the leaf surface, E_v the transpiration and E_c the direct evaporation from wet leaf surfaces. The ground temperature is calculated from the ground surface energy balance.

[11] The aerodynamic resistances for momentum and heat transfer are calculated using the surface layer similarity theory for the eddy diffusivity. The subcanopy resistance for the heat and moisture fluxes between the soil surface and the lowest canopy layer and between canopy layers is estimated as

$$R_k = \int \frac{dz}{K_h}. \tag{6}$$

The eddy diffusivity within the canopy layer for temperature and moisture is assumed to decrease exponentially from the canopy top downward toward the ground surface [*Bonan*, 1996]

$$K_h = K_{sfc} \exp\left(-\alpha\left(1 - \frac{z}{H}\right)\right), \tag{7}$$

where K_{sfc} is the eddy diffusivity at the canopy top calculated from Monin-Obukhov similarity, α is a non-dimensional constant, z is the height above ground and H is the canopy height.

[12] The leaf boundary layer resistance is calculated as in the work of *Jones* [1992]

$$R_b = 100(d/u)^{0.5}, \tag{8}$$

where d is the characteristic dimension of leaf and u is the wind speed in each canopy layer. The default value of 0.08 m from *Williams et al.* [1996] is used for d in this study. The wind profile within the canopy is assumed to decrease exponentially downward as

$$U(z) = U_c \exp\left(-\alpha\left(1 - \frac{z}{H}\right)\right), \tag{9}$$

where U_c is the wind speed at the canopy top.

2.2. Surface Organic Layer

[13] The topsoil layer is generalized to include organic content. The thermal conductivity is computed as

$$K = \Sigma K_i f_i, \tag{10}$$

where K_i is the thermal conductivity of each material component (Table 1) and f_i is the volume fraction of each material. The volumetric heat capacity of the topsoil layer, C (J K^{-1} m^{-3}) is represented as

$$C = \Sigma C_i f_i, \tag{11}$$

where C_i is the volumetric heat capacity of the i_{th} soil component. For the thermal conductivity of the mineral soil, Johansen's parameterization [*Peters-Lidard et al.*, 1998] is used.

[14] For soil evaporation, we adopted the commonly used expression

$$E = \beta E_p, \tag{12}$$

where E_p is potential evaporation, which is calculated by a Penman-based energy balance approach and β is calculated as

$$\beta = \frac{\Theta_1 - \Theta_w}{\Theta_s - \Theta_w}, \tag{13}$$

where Θ_s is saturation soil moisture, Θ_1 is soil moisture at first soil layer and Θ_w is the wilting point.

[15] The organic soil has a small bulk density, typically about 0.13 g cm^{-3}, while mineral soil has a typical value of about 1.3 g cm^{-3} for the BOREAS sites [*Halliwell and Apps*, 1997]. The organic material usually includes highly permeable fibric peat near the surface [*Letts et al.*, 2000], which dries out quickly, corresponding to rapidly decreasing hydraulic conductivity and decreasing surface evaporation. To include this effect into the above formulation, we used the following values as the saturation point and wilting point.

$$\Theta_s = 0.87 \tag{14}$$

$$\Theta_w = 0.22 \tag{15}$$

The saturation point is based on bulk density and wilting point is used as a tuning parameter rather than pure physical quantity. A similar approach was employed by *Pauwels and Wood* [1999a, 1999b] where the soil resistance was calibrated for each tower site to represent the reduction of evaporation from a surface moss layer.

3. Data

[16] We compared the land surface model with eddy correlation data collected at 39 m on the old aspen tower in BOREAS 1994 and at 4 m on a small tower approximately 40 m from the main tower. The study site (56.629°*N* 106.200°*W*) was located in Prince Albert National Park, approximately 50 km NNW of Prince Albert, Saskatchewan, Canada. The site lies near the southern limit of the boreal forest with the transition to parkland occurring approximately 15 km to the southwest. The soil texture is sandy loam covered by about 8 cm of organic material. A natural fire occurred approximately 70 years ago resulting in an even aged stand of

Table 1. Thermal Properties of Soil Constituents From *Farouki* [1986]

Material	Heat Capacity, $\times 10^3 J K^{-1} m^{-3}$	Thermal Conductivity, $W m^{-1} K^{-1}$
Quartz	1942	8.4
Soil minerals	1942	2.9
Soil organics	2503	0.25
Water	4186	0.6
Ice	1883	2.5
Air	1.2	0.026

aspen with a mean canopy height of 21.5 m and mean diameter at the 1.3 m height of 20 cm. Crown space was limited to the upper 5–6 m, beneath which was a branchless trunk space. The understory was dominated by a uniform cover of hazelnut with a mean height of 2 m. The fetch was at least 3 km in all directions.

[17] Two periods were selected for model evaluation and sensitivity tests during which skies were mostly clear except for a few short rain events. The characteristics of the two periods are described in Table 2. The first period is pre-leaf-out and snow free. According to *Blanken et al.* [1997], the leaf-out began in the third week of May. The second period is well after full leaf-out when the leaf area index (LAI) was approximately constant with time. The parameters used in SPA are listed in Table 3. To force the model in an offline mode, we used meteorology data observed at 39 m on the main tower [*Hartog and Neumann*, 2000], precipitation and longwave radiation from the Airborne Fluxes and Meteorology data set [*Osborne et al.*, 1998] and observed soil data from *Black* [2000]. The model time step is 15 min. Meteorological forcing data are available at 30-min intervals, and precipitation and longwave radiation are available at 15-min intervals. We have interpolated meteorological forcing data into 15-min intervals.

[18] While we consider the data to be the "truth" for evaluation of the model, we must recognize a variety of errors. Random flux errors for individual 30-min. records may be greater than 10% and often greater than 20% for nonstationary transition periods and some nocturnal periods [*Mahrt*, 1998]. Subcanopy measurements may be influenced by subcanopy heterogeneity. Measurements of wind and temperature in the subcanopy are not representative of the entire subcanopy layer particularly at night when a strong surface inversion generally forms in the lowest 5 m [*Mahrt et al.*, 2000].

[19] *Nakamura and Mahrt* [2001] found that the above-canopy eddy correlation measurements in BOREAS were generally within the roughness sublayer, below the surface layer where Monin-Obukhov similarity theory applies. Model uses Monin-Obukhov similarity theory, which generally underestimates mixing in the roughness sublayer. As a probable consequence, the observed vertical temperature difference between the two observational levels (13 m, 39 m) is significantly smaller than that predicted using Monin-Obukhov similarity theory (Figure 2), especially in stable conditions, implying greater mixing compared to Monin-Obukhov similarity theory. The influence of the height dependence of the footprint on the observed vertical temperature difference and fluxes cannot be assessed here, which is always a concern in the roughness sublayer.

4. Comparison With Aspen Data

[20] The model was run for two 10-day periods, one in the pre-leaf-out and the other in the post-leaf-out period.

4.1. Pre-Leaf-Out Period

[21] Comparison of the 10-day averaged diurnal cycle between the model and the observations (Figure 3) indicates that the above-canopy and understory fluxes are simulated by the model reasonably well during the pre-leaf-out period, with some exceptions. Table 4 shows the statistical comparisons between model-derived and tower-observed fluxes. Because of the small LAI during this period, the total latent heat flux is dominated by soil evaporation. The relatively low correlation between the model and observed evaporation (Table 4) is due to poor model simulation of the direct evaporation from the soil immediately after rainfall. Although the rainfall amount is small, the observed subcanopy moisture flux, including direct evaporation from the soil and canopy, reaches about 200 Wm^{-2} immediately after rainfall.

[22] The observed sensible heat flux of nearly 150 Wm^{-2} in the subcanopy for the pre-leaf-out period implies significant buoyancy-generation of turbulence energy within the subcanopy. In sparse canopies with low LAI, the use of the usual constant extinction coefficient (equation (7)) can underestimate turbulent mixing within the canopy, resulting in larger vertical temperature gradients in the subcanopy and higher ground surface temperature than observed during daytime. The model shows a warm bias in 4-m subcanopy temperature during daytime (Figure 3), consistent with underestimation of mixing, although advection and errors in the model radiative transfer could also be factors. The apparent cold bias in the nocturnal subcanopy, could be partly due to the location of the observed temperature near the top of a strong surface inversion of about 5-m depth. Since the model does not consider subcanopy stability in the heat transfer in the subcanopy, the model does not capture the strong nocturnal surface inversion, which results in overestimation of the understory sensible heat flux.

4.2. Post-Leaf-Out Period

[23] The post-leaf-out period is characterized by a significantly higher LAI and lower soil moisture content than in the pre-leaf-out period (Table 2). The simulated latent heat flux and soil heat flux are generally close to the observed values (Figure 4), although the understory latent heat flux is overestimated by 30 Wm^{-2} during the late afternoon from 1500 LST to 1800 LST. The transpiration is controlled by the leaf boundary layer resistance and the stomatal resistance. In unstable conditions with significant wind, the leaf boundary layer resistance is usually smaller than the sto-

Table 2. Characteristics of Selected Periods

	Period	PAI(LAI)[a] Hazelnut/Aspen	Initial Topsoil Moisture
Pre-leaf-out	5–14 May	0.3(0.1)/1.2(0.3)	0.23
Post-leaf-out	30 July to 8 Aug.	3.4(3.2)/3.2(2.3)	0.11

[a]PAI is the plant area index (the sum of leaf area index and stem area index) and LAI is the leaf area index.

Table 3. Model Parameters

Parameter	Value	Unit	Source
Stem specific hydraulic Conductivity	20	m, mol, m^{-1}, s^{-1}, MPa^{-1}	estimated
Root resistivity	50	MPa s g $mmol^{-1}$	estimated
Total fine root biomass	657	g m^{-2}	*Steele et al.* [1997]
Canopy layer capacitance	8000	mmol MPa^{-1}	*Williams et al.* [1996]
Minimum leaf water potential	−2.3	MPa	*Kimball et al.* [1997]
RuBP carboxylation catalytic Rate coefficient at 30°C κ_c	37.8	μ mol g^{-1} N s^{-1}	*Williams et al.* [2001]
Electron transport rate Coefficient at 30°C κ_j	49.0	μ mol g^{-1} N s^{-1}	*Williams et al.* [2001]
Soil color	4	no unit	*Kimball et al.* [1997]

matal resistance. Therefore the transpiration is limited by stomatal resistance and is less sensitive to leaf boundary layer resistance. However, when the wind speed is weak, transpiration can be more limited by the leaf-boundary layer resistance. In late afternoon when the subcanopy air becomes stably stratified, the wind speed within the canopy becomes weak due to less downward transport of momentum. The overestimation of subcanopy wind speed causes underestimation of leaf boundary layer resistance, which causes overestimation of transpiration in late afternoon.

[24] Model errors for the sensible heat flux are greater than those for the latent heat flux. The model overestimates the subcanopy sensible heat flux throughout the diurnal period (Figure 4 and Table 4), possibly due to failure to resolve the vertical structure of the understory. The model employs only two layers of vegetation for application in regional models. The two vegetation layers, here each 10 m deep, assume uniform plant distribution within each layer whereas the actual vertical distribution includes a thick overstory of 5–6 m thickness and a 2-m dense understory near ground. The layer-averaged resistance in the lower canopy layer underestimates the leaf boundary layer resistance for the 2-m understory and therefore overestimates the subcanopy sensible heat flux from the understory. Note that transpiration is less sensitive to leaf boundary layer resistance since it is limited by stomatal conductance in unstable conditions, compared to sensible heat flux that depends more on leaf boundary layer resistance.

[25] In the transition periods with low sun angle, the modeled subcanopy is stably stratified while the atmosphere above the canopy is still unstably stratified. The subcanopy mixing in the model depends on the stability above the canopy and therefore does not recognize the difference between the stability above and within the canopy. As a result, the model incorrectly predicts large negative sensible heat flux in the subcanopy during the transition periods whereas the observed subcanopy heat flux is small (Figure 4).

[26] The model overestimates the daytime sensible heat flux above the canopy by 50 W m^{-2}. This overestimation could be due to omission of the heat storage within the canopy and advection of temperature.

[27] The simulated soil heat flux agrees with the observations reasonably well during the day, but is overpredicted at night (Figure 4). The modeled temperature at the 4-m level is in good agreement with the observed temperature during the day but it is too cool at night giving larger temperature gradient than that observed in the upper canopy. The apparent cold bias could be due to location of the observed temperature just above the subcanopy surface inversion (section 4.1) or could be due to model overestimation of the radiative cooling of leaves.

[28] The leaf radiative cooling is coupled to the leaf boundary layer resistance (equation (8)) through its influence on leaf temperature in the leaf energy balance. The leaf boundary layer resistance represents the transfer of heat and moisture between the leaf surface and adjacent air and in the model is only a function of wind speed. In unstable conditions, the mixing in the canopy is significant, such that the canopy wind speed and air temperature are close to those adjacent to the leaf surface. However, in stable conditions, large differences exist between average canopy wind speed and air temperature and wind speed and air temperature adjacent to the leaf surface due to suppression of mixing by the stable stratification. Without consideration of these differences, the heat exchange between the leaf and the atmosphere is overestimated in stable conditions, which reduces the temperature difference between the radiatively cooled leaf surface and the air. The resulting overprediction of leaf temperature causes more emitted longwave radiation and therefore larger net radiative cooling of the canopy. Due to the overcooling in the subcanopy, the subcanopy air temperature decreases to the saturation point causing overestimation of understory condensation (Figure 4).

5. Influence of Organic Material

[29] To examine the effect of the surface organic layer on the subcanopy processes, simulations were performed with and without organic material in the upper soil layer. During

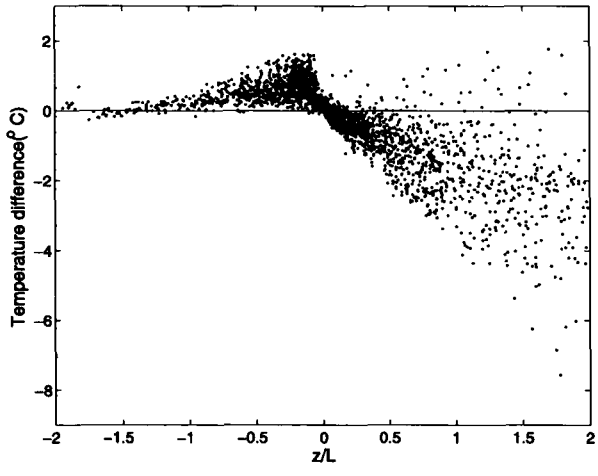

Figure 2. The modeled vertical temperature difference ($T_{13m} - T_{39m}$) minus the observed vertical temperature difference between the displacement height (13 m) and reference height (39 m) as a function of z/L.

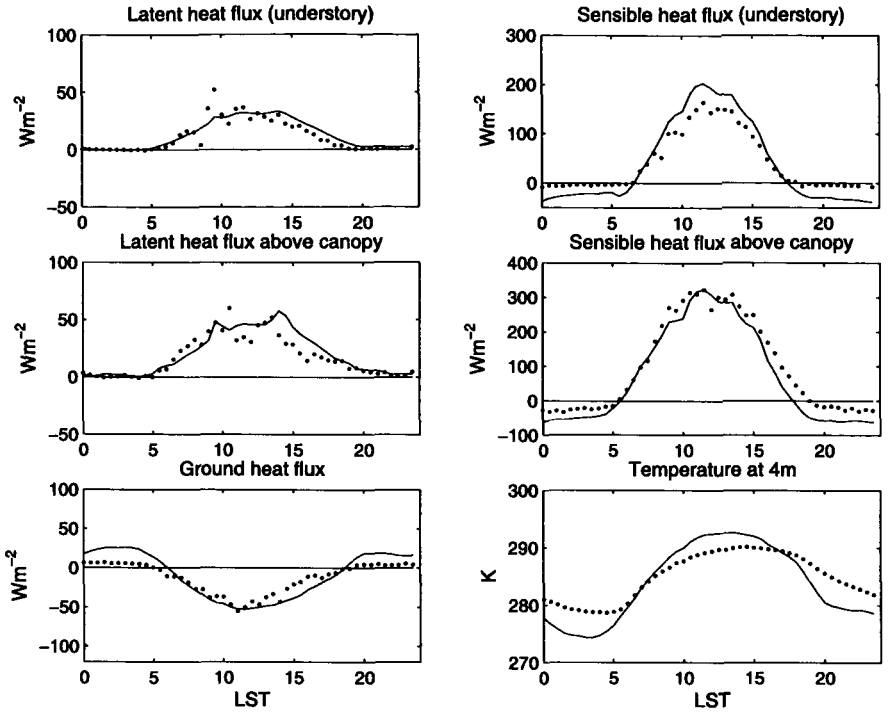

Figure 3. Composite diurnal variation for the observed (circles) and modeled (solid line) variables for the pre-leaf-out period.

the pre-leaf-out period, the simulation with no organic material substantially overestimates soil evaporation and heat flux into the ground and underestimates understory sensible heat flux (Figure 5). The simulation with organic material predicts fluxes much closer to the observed values. The unrealistically large soil evaporation in the simulation with no organic material leads to rapid drying of the soil. The organic material acts as a partial insulator between the soil surface and deep soil. As a result, the surface organic layer makes the subcanopy more unstable during daytime and more stable during night. This improves the comparison with the observations.

[30] The impact of the organic material is smaller after leaf-out because the understory reduces exchange between the ground and the atmosphere (Figure 6). The overestimation of soil evaporation in the simulation without an organic layer leads to underestimation of the vapor pressure deficit in the subcanopy, which in turn leads to underestimation of transpiration. Therefore the sensitivity of latent heat flux to the organic layer is reduced. The simulation with no organic material also overestimates the downward ground heat flux during the daytime, which results in smaller sensible heat flux in the subcanopy.

6. Conclusions

[31] The land surface scheme tested in this study roughly captures the main energy partition between the understory

Table 4. Results of Model Application[a]

Period	Variable	Mean Observation, W m^{-2}	Mean Simulation, W m^{-2}	R, Dimensionless	RMSE, W m^{-2}
Pre-leaf-out					
	H_u	40.62	40.65	0.96	33.62
	H_a	96.51	71.76	0.95	54.71
	LE_u	11.37	12.69	0.62	15.48
	LE_a	17.06	19.76	0.59	21.62
	G	−12.36	−9.00	0.92	14.35
Post-leaf-out					
	H_u	2.39	−0.51	0.69	11.48
	H_a	10.15	4.63	0.88	35.30
	LE_u	21.46	23.76	0.81	23.6
	LE_a	78.02	74.49	0.93	36.42
	G	−5.03	−2.52	0.95	5.29

[a]Subscripts u and a represent understory and above the canopy respectively, R is the correlation coefficient and RMSE is the root mean square error.

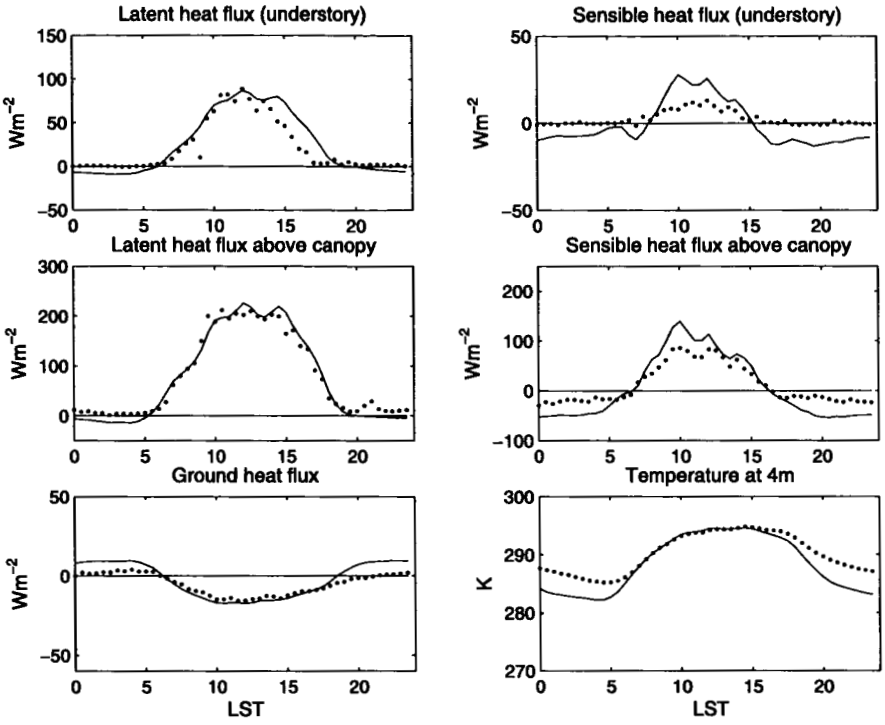

Figure 4. Composite diurnal variation for the observed (circles) and modeled (solid line) variables for the post-leaf-out period.

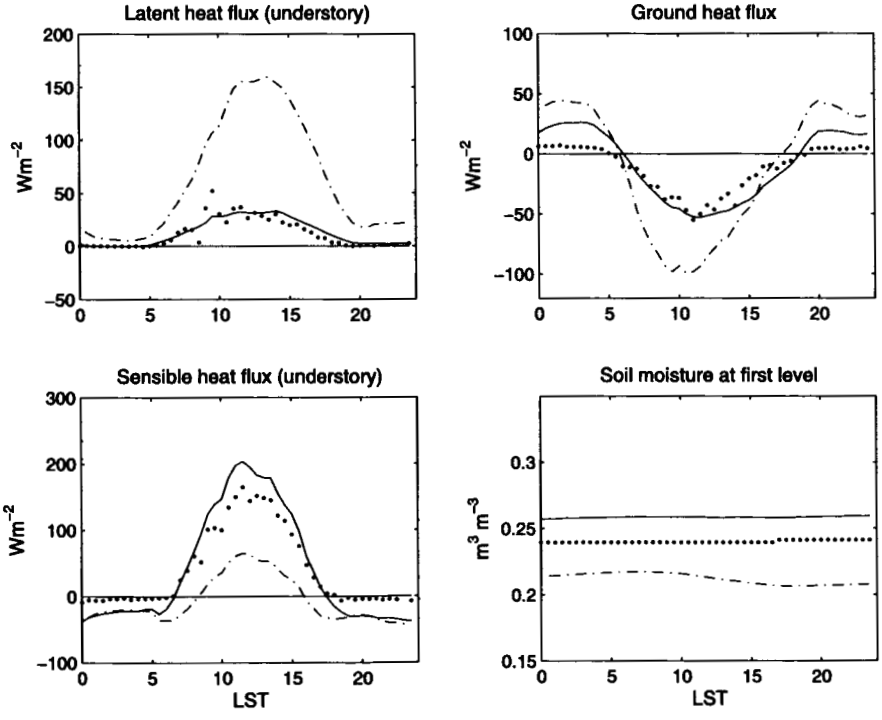

Figure 5. Comparison between the model with (solid line) and without (dash-dot line) the organic layer for the pre-leaf-out period and the observed values (circles).

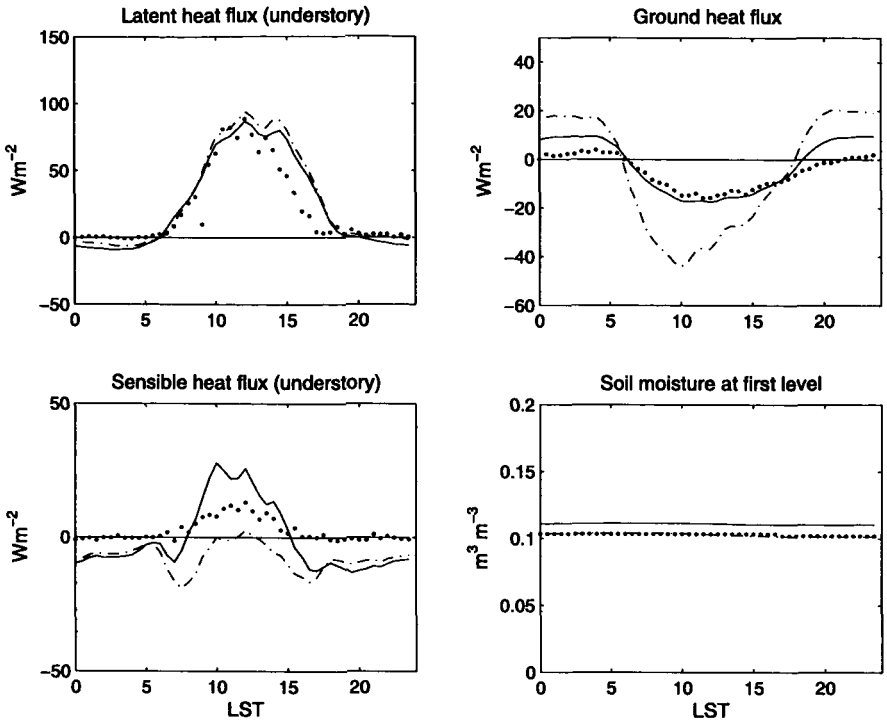

Figure 6. Comparison between the model with (solid) and without (dash-dot line) the organic layer for the post-leaf-out period and the observed values (circles).

and overstory during both pre-leaf-out and post-leaf-out periods. The model also partitions the net energy into latent heat flux and sensible heat flux reasonably well, provided that the modeled upper soil layer includes organic material. Failure to include such material causes substantial overestimation of soil evaporation and subsequent errors in the subcanopy fluxes, particularly prior to leaf-out. The organic material reduces the heat exchange between the ground surface and deeper soil, which makes the subcanopy more stable at night and more unstable during the daytime.

[32] Because of complex interactions between different components of the canopy-ground system, isolating the cause of other errors is difficult without detailed observations of individual processes. For example, underestimation of the leaf boundary layer resistance at night causes overestimation of the transfer of heat from the canopy air to the leaf surface, which leads to overestimation of leaf temperature and overestimation of radiative energy loss from the canopy system. Other errors include overestimation of mixing in the understory due to failure to resolve the vertical structure of the understory.

[33] The model does not directly include the important influence of diurnal variation of subcanopy stability on the mixing. This omission appears to cause overestimation of exchange between the ground and subcanopy air in transition periods and at night when an inversion layer forms in the subcanopy. We are currently examining this influence using data from a variety of open canopies.

[34] **Acknowledgments.** We gratefully acknowledge the collection of data at the aspen site by Andy Black, Xuhui Lee, Ralf Staebler and coworkers. The comments of Jielun Sun, Hank Loesher and two anonymous reviewers are gratefully appreciated. This work was supported by Grant NAG5-11231 from the NASA Terrestrial Ecology Program and Grant 0107617-ATM from the Physical Meteorology Program of the National Sciences Foundation and by the Post-doctoral Fellowship Program of Korea Science and Engineering Foundation (KOSEF).

References

Albertson, J. D., G. G. Katul, and P. Wiberg (2001), Relative importance of local and regional controls on coupled water, carbon, and energy fluxes, *Adv. Water Resour.*, *102*, 1103–1118.

Amthor, J. S. (1994), Scaling CO_2-photosynthesis relationships from the leaf to the canopy, *Photosyn. Res.*, *39*, 321–350.

Amthor, J. S., M. L. Goulden, J. W. Munger, and S. C. Wofsy (1994), Testing a mechanistic model of forest-canopy mass and energy exchange using eddy correlation: Carbon dioxide and ozone uptake by a mixed oak-maple stand, *Aust. J. Plant Physiol.*, *21*, 623–651.

Black, T. A. (2000), BOREAS TF-01 SSA-OA understory flux: Meteorological and soil temperature data, Data set, http://www.daac.ornl.gov, Oak Ridge Natl. Lab., Oak Ridge, Tenn.

Blanken, P. D., T. A. Black, P. C. Yang, H. H. Neumann, Z. Nesic, R. Staebler, G. den Hartog, M. D. Novak, and X. Lee (1997), Energy balance and canopy conductance of a boreal aspen forest: Partitioning overstory and understory components, *J. Geophys. Res.*, *102*, 28,915–28,927.

Bonan, G. B. (1996), A land surface model (LSM version 1.0) for ecological, hydrological and atmospheric studies: Technical description and user's guide, *NCAR Tech. Note NCAR/TN-417+STR*, Natl. Cent. for Clim. Res., Boulder, Colo.

Cellier, P., and Y. Brunet (1991), Flux-gradient relationships above tall plant canopies, *Agric. Forest Meteorol.*, *58*, 93–117.

Choudhury, B. J., and J. L. Monteith (1988), Four layer model for the heat budget of homogeneous land surfaces, *Q. J. R. Meteorol. Soc.*, *114*, 373–398.

Cotton, W. R., et al. (2003), RAMS 2001: Current status and future directions, *Meteorol. Atmos. Phys.*, *82*, 5–29.

Dolman, A. J., and J. S. Wallace (1991), Lagrangian and K-theory approaches in modelling evaporation form sparse canopies, *Q. J. R. Meteorol. Soc.*, *117*, 1325–1340.

Farouki, O. T. (1986), *Thermal Properties of Soils, Ser. on Rock and Soil Mech.*, vol. 11, 136 pp., Trans Tech, Claustal-Zellerfeld, Germany.

Halliwell, D. H., and M. J. Apps (1997), Boreal Ecosystem-Atmosphere Study (BOREAS) biometry and auxiliary sites (soil and detritus data) version 3.02, Can. Forest Serv., Northern Forestry Cent., Edmonton, Alberta.

Hartog, G. D., and H. Neumann (2000), BOREAS TF-02 SSA-OA tower flux: Meteorological and precipitation data, Data set, http://www.daac.ornl.gov, Oak Ridge Natl. Lab., Oak Ridge, Tenn.

Jones, H. G. (1992), *Plants and Microclimate*, Cambridge Univ. Press, New York.

Kaimal, J. C., and J. J. Finnigan (1994), *Atmospheric Boundary Layer Flows*, Oxford Univ. Press, New York.

Katul, G. G., and J. D. Albertson (1998), An investigation of higher-order closure models for a forested canopy, *Boundary Layer Meteorol.*, *89*, 47–74.

Katul, G., et al. (1999), Spatial variability of turbulent fluxes in the roughness sublayer of an even-aged pine forest, *Boundary Layer Meteorol.*, *93*, 1–28.

Kimball, J. S., P. E. Thornton, M. A. White, and S. W. Running (1997), Simulating forest productivity and surface—Atmosphere carbon exchange in the BOREAS study region, *Tree Physiol.*, *17*, 589–599.

Koren, V. I., J. Schaake, K. Mitchell, Q.-Y. Duan, F. Chen, and J. M. Baker (1999), A parameterization of snowpack and frozen ground intended for NCEP weather and climate models, *J. Geophys. Res.*, *104*, 19,569–19,585.

Kustas, W. P. (1990), Estimates of evapotranspiration with a one and two layer model of heat transfer over partial canopy cover, *J. Appl. Meteorol.*, *29*, 704–715.

Letts, M. G., N. T. Roulet, N. T. Comer, M. R. Skarupa, and D. L. Verseghy (2000), Parameterization of peatland hydraulic properties for the Canadian Land Surface Scheme, *Atmos. Ocean*, *38*, 141–160.

Mahrt, L. (1998), Flux sampling errors for aircraft and towers, *J. Atmos. Oceanic Technol.*, *15*, 416–429.

Mahrt, L., and H. L. Pan (1984), A two-layer model of soil hydrology, *Boundary Layer Meteorol.*, *29*, 1–20.

Mahrt, L., X. Lee, A. Black, H. Neumann, and R. M. Staebler (2000), Nocturnal mixing in a forest subcanopy, *Agric. Forest Meteorol.*, *101*, 67–78.

Nakamura, R., and L. Mahrt (2001), Roughness lengths and similarity theory for local and spatially averaged fluxes, *Agric. Forest Meteorol.*, *100*, 47–61.

Norman, J. M., W. P. Kustas, and K. S. Humes (1995), Source approach for estimating soil and vegetation energy fluxes in observations of directional radiometric surface temperature, *Agric. Forest Meteorol.*, *77*, 263–293.

Osborne, H., K. Yound, V. Wittrock, and S. Shewchuck (1998), BOREAS/SRC AMS suite b surface meteorological and radiation data: 1994, Data set, http://www.daac.ornl.gov, Oak Ridge Natl. Lab., Oak Ridge, Tenn.

Pauwels, V. R. N., and E. F. Wood (1999a), A soil-vegetation-atmosphere transfer scheme for the modeling of water and energy balance processes in high latitude: 1. Model improvements, *J. Geophys. Res.*, *104*(D22), 27,811–27,822.

Pauwels, V. R. N., and E. F. Wood (1999b), A soil-vegetation-atmosphere transfer scheme for the modeling of water and energy balance processes in high latitude: 2. Application and validation, *J. Geophys. Res.*, *104*(D22), 27,823–27,839.

Pauwels, V. R. N., and E. F. Wood (2000), The importance of classification differences and spatial resolution of land cover data in the uncertainty in model results over boreal ecosystems, *J. Hydrometeorol.*, *1*, 255–266.

Peters-Lidard, C. D., E. Blackburn, X. Liang, and E. F. Wood (1998), The effect of soil thermal conductivity parameterization on surface energy fluxes and temperatures, *J. Atmos. Sci.*, *55*, 1209–1224.

Physick, W., and J. R. Garratt (1995), Incorporation of a high-roughness lower boundary into a mesoscale model for studies of dry deposition over complex terrain, *Boundary Layer Meteorol.*, *74*, 55–71.

Raupach, M. R., and J. J. Finnigan (1988), Single layer models of evaporation from plant canopies are incorrect but useful, whereas multi-layer models are correct but useless: Discuss, *Aust. J. Plant Physiol.*, *15*, 705–716.

Raupach, M. R., J. J. Finnigan, and Y. Brunet (1996), Coherent eddies and turbulence in vegetation canopies: The mixing-layer analogy, *Boundary Layer Meteorol.*, *78*, 351–382.

Schaake, J. C., V. I. Koren, Q. Y. Duan, K. Mitchell, and F. Chen (1996), A simple water balance model (SWB) for estimating runoff at different spatial and temporal scales, *J. Geophys. Res.*, *101*, 7461–7475.

Sellers, P. J., Y. Mintz, Y. C. Sud, and A. Dalcher (1986), A simple biosphere model (SiB) for use within general circulation models, *J. Atmos. Sci.*, *43*, 505–531.

Sellers, P., et al. (1995), The boreal ecosystem—Atmosphere study (BOREAS): An overview and early results from the 1994 field year, *Bull. Am. Meteorol. Soc.*, *76*, 1549–1577.

Shaw, R. H., and U. Schumann (1992), Large-eddy simulations of turbulent flow above and within a forest, *Boundary Layer Meteorol.*, *61*, 47–64.

Simpson, I. J., G. W. Thurtell, H. H. Neumann, G. Den Hartog, and G. C. Edwards (1998), The validity of similarity theory in the roughness sublayer above forests, *Boundary Layer Meteorol.*, *87*, 69–99.

Steele, S. J., S. T. Gower, J. G. Vogel, and J. M. Norman (1997), Root mass, net primary production and turnover in aspen, jack pine and black spruce forests in Saskatchewan and Manitoba, Canada, *Tree Physiol.*, *17*, 577–587.

Su, H. B., K. T. Paw, and R. H. Shaw (1996), Development of a coupled leaf and canopy model for the simulation of plant-atmosphere interaction, *J. Appl. Meteorol.*, *35*, 733–748.

Sun, J., W. Massman, and D. Grantz (1999), Aerodynamic variables in the bulk formulation of turbulent fluxes, *Boundary Layer Meteorol.*, *91*, 109–125.

Van de Wiel, B. J. H., R. J. Ronda, A. F. Moene, H. A. R. De Bruin, and A. A. M. Holtslag (2002), Intermittent turbulence and oscillations in the stable boundary layer over land. Part I: A bulk model, *J. Atmos. Sci.*, *59*, 942–958.

Wenzel, A., N. Kalthoff, and V. Horlacher (1997), On the profiles of wind velocity in the roughness sublayer above a coniferous forest, *Boundary Layer Meteorol.*, *84*, 219–230.

Williams, M., E. B. Rastetter, D. N. Fernades, M. L. Goulden, S. C. Wofsy, G. R. Shaver, J. M. Melillo, J. W. Munger, S. M. Fan, and K. J. Nadelhoffer (1996), Modelling the soil-plant-atmosphere continuum in a Quercus-Acerstand at Harvard forest: The regulation of stomatal conductance by a light, nitrogen and soil/plant hydraulic properties, *Plant Cell Environ.*, *19*, 911–927.

Williams, M., B. E. Law, P. M. Anthoni, and M. Unsworth (2001), Use of a simulation model and ecosystem flux data to examine carbon-water interactions in ponderosa pine, *Tree Physiol.*, *21*, 287–298.

Y.-H. Lee, Department of Astronomy and Atmospheric Sciences, Kyungpook National University, Daegu 702-701, Republic of Korea. (young@knu.ac.kr)

L. Mahrt, College of Oceanic and Atmospheric Sciences, Oregon State University, Corvallis, OR 97331, USA. (mahrt@coas.oregonstate.edu)